Enhancement of High Dynamic Range Images Using Variational Calculus Regularizer with Stochastic Resonance

Sumit Kumar
Indian Institute of Technology Patna
sumitphd13@gmail.com

Rajib Kumar Jha
Indian Institute of Technology Patna
jharajib@gmail.com

ABSTRACT

While capturing pictures by a simple camera in a scene with the presence of harsh or strong lighting like a full sunny day, we often find loss of highlight detail information (overexposure) in the bright regions and loss of shadow detail information (underexposure) in dark regions. In this manuscript, a classical method for retrieval of minute information from the high dynamic range image has been proposed. Our technique is based on variational calculus and dynamic stochastic resonance (DSR). We use a regularizer function, which has been added in order to optimise the correct estimation of the lost details from the overexposed or underexposed region of the image. We suppress the dynamic range of the luminance image by attenuating large gradient with the large magnitude and low gradient with low magnitude. At the same time, dynamic stochastic resonance (DSR) has been used to improve the underexposed region of the image. The experimental results of our proposed technique are capable of enhancing the quality of images in both overexposed and underexposed regions. The proposed technique is compared with most of the state-of-the-art techniques and it has been observed that the proposed technique is better or at most comparable to the existing techniques.

Keywords

Dynamic stochastic resonance (DSR), wavelet, variational calculus, regularizer, gradient, tone mapping

1. INTRODUCTION

In the digital photography technology, **exposure** actually controls the quantity of light that can reach the image sensor and the **lightness** [1, 2, 3], which is a very important parameter, is basically the amount of light which is shown by the image. There is always physical limitation related to the intensity or luminance that a camera can hold or capture, is technically called as **dynamic range**. An outdoor image with strong or weak lighting generally has a much large dynamic range than the bearing capability of an image sensor , which causes the loss of highlight/shadow details in the photograph captured by the camera. It can be well understood by the much difference in the dynamic range of the digital camera and the outdoor scenes, which is shown in Fig. 1.

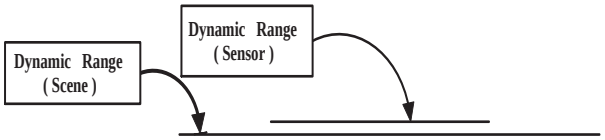

Figure 1: Comparison of dynamic range of scene and sensor

The dynamic range of a regular digital sensor or camera is about $10^3 : 1$, whereas the dynamic range of the natural outdoor scene in full sunny day ranges from 10^5 *to* $10^9 : 1$. When these natural scenes having a high dynamic range (HDR) are captured by the camera with low dynamic range (LDR), bright regions are put as **white**, which is termed as **overexposure**; and some regions with low-intensity values becomes too much **dark**, which is described as **underexposure** . In other words, the lightness values of the overexposed regions are clipped at the maximum values in such a way it only shows white colour, as the colour of the all three components (R, G, B) also becomes maximum. In a similar manner, lightness value of underexposed region are too small and goes to zero. However, high dynamic range (HDR) images are preferred over standard low dynamic range images, and several applications have been demonstrated where such images are extremely useful. But various common display devices (monitors, printers, *etc.*) clip the highly exposed regions. The behaviour of hardware is not able to cope up with the changes in a dynamic range of natural scenes. In other words, we can say that information hidden because of presence of much lightness needs the retrieval of the minute data from an image. The intensity of the overexposed regions is clipped at the maximum value (*i.e.,* 255 in images with 8-bit in every channel), and obviously appears uniformly white. Because of this overexposure, the minute textures get hidden. To preserve the texture, we need to process the gradient of the image and that is the reason we call this method as the gradient processing method. Therefore, it is very obvious that we need to differentiate between the overexposed region because of ample quantity of sunlight and natural lightness regions. High dynamic range (HDR) radiance maps are very popular and common in computer graphics. However, we need to convert it into low dynamic range so that its visuality can be enhanced. Sometimes, un-

ICVGIP, December 18-22, 2016, Guwahati, India

DOI: http://dx.doi.org/10.1145/3009977.3010039

derexposure is the major issue. So, we have used dynamic stochastic resonance [4, 5] to enhance the visuality of the underexposed regions. Mathematically, the main aim of image processing and analysis is to recover the original non-noisy image P from the observed noisy image I, where P and I represents pure and impure image respectively.

$$I = RP + \eta, \tag{1}$$

where R is a linear operator and η is noise. The Eq. 1 clearly mentions that the recovery of P from I is not so easy and it is not sufficient to make sure about the existence, uniqueness and stability of P from I. It is therefore required to regularise the given problem by adding some extra constraint on the solution. we discuss this in detail in later section.

In this paper, Section 2 deals with the discussion about the works carried out by different research groups. A brief investigation has been made for its mathematical approach in Section 3. Section 4 describes the approach for the simulation and implementation . Results have been presented in Section 5. The direction about the future work has been mentioned in Section 6.

2. PEER REVIEW

The over-/underexposure region is created when the dynamic range of a scene is very much higher than the dynamic range of the sensor or camera. Consequently, the minute information of the overexposed regions are completely overridden by only white colour. Similarly, in the underexposed regions, minute information is covered by black spots. The colour detection and correction are one of the challenging tasks because to differentiate between the overexposed region (a colour region created because of sensor limitation), and the natural white region of the image is difficult. In the few decades, there have been tremendous works for displaying high dynamic range images on low dynamic range devices. Many techniques have been developed for colour image restoration process. The very appropriate work which addresses the overexposure correction is done by Zhang and Brainard [6] and Masood et al. [7]. Zhang and Brainard used the ratios between different colour channels in order to recover the overexposed channels based on the pixels around the overexposed region in a spatial domain. However, the applicability of this spatial-invariant is not possible in real cases. Thus, Masood et al. estimated pixel values in the overexposed channel using spatial-variant ratios. However, the major drawback related to both the method is that it can handle partial overexposure *i.e.,* image having one or two channels. Wang et al. [8] described texture synthesis algorithm in order to find out the detail texture in overexposed regions and the lightness is estimated by a Gaussian ellipsoid which is based on the pixels of the neighbours around the overexposed region. A lot of works have to be done if there are many small overexposed regions. In [9, 10, 11], high dynamic range imaging can be compressed into a low dynamic range image. They described different methods which can easily extract the details of overexposed regions using Near-Infrared Ranging (NIR) image. This method can also deal with the motion. But the major drawback with this method is that it needs special equipments, which is a panic situation. One of the very popular methods called as histogram equalisation [12, 13], which is used for image enhancement. It spreads out most frequent intensity values in order to adjust the image intensities. This permits the low contrast to gain a higher contrast. However, this method is appropriate for the images whose foreground and background are either both dark or both bright. It does not work well for the images which contains both dark and bright regions simultaneously. In the paper [14], they have discussed the Poisson image editing which can be applied for tone mapping, contrast enhancement, shadow removal, *etc.* It approximates the image gradient to minimise the effect of non-uniform illuminance preserving all fine details. There are many representative methods to deal with the over/under exposure regions. For example, PDE-based variational method, the total variation (TV)- based regularisation [15, 16] and template-based approach [17] where the damaged regions are covered by some similar patches of undamaged regions. The tone mapping technique proposed by Fattal et al. [10] is adopted for a dynamic range compression of the luminance component of the image.

3. MATHEMATICAL REVIEW

3.1 Variational Calculus

In the continuous variable domain, a pure image P and the noisy or high dynamic range image [18] I can be shown by the function of $\Omega \subset R^2 \rightarrow R$ which is related to the every pixel value either in gray level or in any colour plane. In the image, the levels are fixed numbers and have been mapped as $0 \leq P(x,y) \leq 1 \quad \forall (x,y) \in \Omega$. The model proposed by Geman [19] for image reconstruction leads to search for a solution among the minima of the energy of the noise. Lowering the presence of noise can be interpreted by minimising its energy

$$L_\alpha(P) = \int_\Omega \left(I(x,y) - RP(x,y)\right)^2 dxdy + Regularizer, \tag{2}$$

where Regularizer is very important to achieve the global optimum value.

$$\begin{aligned} L_\alpha(P) = \int_\Omega \left(I(x,y) - RP(x,y)\right)^2 dxdy + \\ \alpha \int_\Omega f(DP(x,y))dxdy, \end{aligned} \tag{3}$$

where the first term represents the energy of noise in full image range. In [19], they have added a regularization term as $\int \left(f\left(\frac{\partial P}{\partial x}\right)\right) + \left(f\left(\frac{\partial P}{\partial y}\right)\right)$. This is invariant under rotation but we have chosen this in such a way that it regularizes to extract the lines and columns. The number $\alpha \in R$ is a parameter which permits us to balance the influence of every integral term in the Eq. 3. If we put $\alpha = 0$, then it becomes

$$L_\alpha(P) = \int_\Omega \left(I(x,y) - RP(x,y)\right)^2 dxdy, \tag{4}$$

which is nothing but energy of the noise and the problem corresponds to the least-square method associated with the Eq. 1. The every solution for the minimum of the Eq. 4 satisfies the the following equation

$$R^* I = R^* RP. \tag{5}$$

The Eq. 5 is an ill-posed problem where R^*R may not be invertible and the solution is very often unstable. To over-

come this difficulty, we try to find the solution in some compactness. We may add a regularization term to the attached data. This method was used by Tikhonov [20]. The de-noisy or reconstructed image must be formed by homogeneous regions, separated by some sharp lines or edges. It means that this must hold the strong variations of gray values. Differentiating the Eq. 3 and equating to zero

$$\frac{-\alpha}{2} div\left(\frac{f'(|DP|)DP}{|DP|}\right) + R^*RP = R^*I. \tag{6}$$

Now with Eq. 6, we will try to acquire some sufficient assumptions on the f in order to save minor edges (less gradients). To do this, for every point where the gradient is non-zero, $V(x,y) = \frac{DP(x,y)}{|DP(x,y)|}$ and $O(x,y)$ is the orthogonal vector to $V(x,y)$. The Eq. 6 can be written as follows

$$\frac{-\alpha}{2}\left(\frac{f'(|DP|)DP}{|DP|}\right) f_{OO} - \frac{-\alpha}{2} P''(|DP|)P_{VV} + R^*RP = R^*I, \tag{7}$$

where $P_{OO} = \frac{1}{|DP|^2}\left(P_x^2 P_{yy} + P_y^2 P_{xx} - 2P_x P_y P_{xy}\right)$ and the term $P_{VV} = \frac{1}{|DP|^2}\left(P_x^2 P_{xx} + P_y^2 P_{yy} + 2P_x P_y P_{xy}\right)$. Because we have to preserve the edge, so we differentiate an edge by some threshold value which has been shown below:

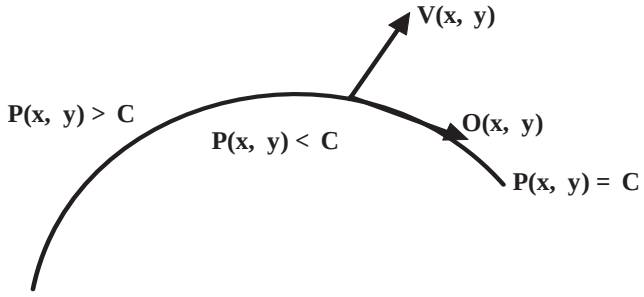

Figure 2: Graph separating two different homogeneous region

Now, if we think about the existence of f'' with the following conditions

$$f'(0) = 0 \quad and \quad f''(0) = 0. \tag{8}$$

$$\frac{-\alpha}{2} f''(0)\left(P_{OO} + P_{VV}\right) + R^*RP = R^*I. \tag{9}$$

Now adding P_{OO} and P_{VV}, we get

$$P_{OO} + P_{VV} = P_{xx} + P_{yy} =\triangle P. \tag{10}$$

Putting the value of $P_{OO} + P_{VV}$ in Eq. 9, it becomes

$$\frac{-\alpha}{2} f''(0)\left(\triangle P\right) + R^*RP = R^*I \tag{11}$$

$$\lim_{t\to\infty} f''(t) = \lim_{t\to\infty} \frac{f'(t)}{t} = 0 \tag{12}$$

$$\lim_{t\to\infty} \frac{f''(t)}{\frac{f'(t)}{t}} = 0 \tag{13}$$

But these are not sufficient conditions to prove that the model is well posed mathematically and it has been discussed in [21]. In order to do this, we suppose that

$$\lim_{t\to\infty} f''(t) = +\infty \tag{14}$$

This growth must not be so strong that it may penalize strong gradients. Hence, we must take linear growth which leads to infinity when $t \to \infty$. Charbonnier [22] shows the choices used in image reconstruction for a comparative study.

3.2 Stochastic Resonance

Noise degrades the performance of any system, but this myth was proved wrong and experimented by Benzi [23] in 1981-82, by exploring the concept of Stochastic Resonance (SR). The phenomenon of stochastic resonance, where the output signals get amplified with the internal noise or externally added noise or both, enhances the signal to noise ratio (SNR). But this enhancement occurs at a certain level of noise. To use the concept of stochastic resonance, the system should hold three basic characteristics: Non-*Linearity*, *Noise* and *weak Input signal*. In a context of image processing, dynamic stochastic resonance represents the transition of high-intensity state to low intensity state. The state transition of a particle in a double-well potential system is based on Brownian motion. The equation of motion of particle in the double well potential system is well described by Langevin's equation

$$\frac{dx(t)}{dt} = \frac{-du(x)}{dx} + \sqrt{D}\zeta(t) \tag{15}$$

where ζ is the friction which is being faced by the moving object. D is the additive noise intensity. The bi-stable potential function $U(x)$ is defined as

$$U(x) = \frac{-ax^2}{2} + \frac{bx^4}{4} \tag{16}$$

where a and b are positive bi-stable parameters defined by $a = 2\sigma_0^2$ and $b < \frac{4a^3}{27}$. This system is stable at one point $x_m = \pm\sqrt{\frac{a}{b}}$ and separated by barrier of height $\triangle U = \frac{a^2}{4b}$, when noise is made to be zero. To make it time dependent, the term $Bsin(\omega t)$ is added. SNR of the system is derived and given by

$$SNR = \left[\frac{4a}{\sqrt{(2)}(\sigma_0\sigma_1)^2}\right] \tag{17}$$

where σ_0 and σ_1 are the standard deviation of the original system and the resonance based system. This increment in the SNR enhances the signal quality. Sometimes, inherent noise is used in wavelet domain [24] for the reconstruction of the signal.

3.3 Algorithm for Enhancement of Underexposed / Overexposed Images

1. Read the high dynamic range image $I(x,y)$
2. Calculate the Luminance of the Image

3. Divide the image into two section **Underexposed region** and **Overexposed region** by thresholding.

4. **Gradient Compression** We have used the same gradient attenuation function as [10] for overexposed Region.

5. Add the regularizer discussed in the Section 3. Here we have discussed two regularizers.

6. Using the discrete wavelet transform for underexposed region, we can have the different frequency components of the image. Apply the wavelet decomposition of the image

   [LL, HL, LH, HH]=**DWT** (Underexposed region)

7. Calculate the different parameters to be used for the application of dynamic stochastic resonance parameters, k, $\triangle t$ as used by Jha. et al. [4].

8. Apply Dynamic Stochastic Resonance on LL of Discrete Wavelet Transform

   $x(n+1) = x(n) + \triangle t\left[ax(n) - bx(n)^3 + LL\right]$

9. Concatenate new LL component of the image and then apply inverse Discrete Wavelet Transform

10. Visuality is the only one bench mark to measure the effectiveness of the algorithm.

4. SIMULATION & IMPLEMENTATION

Our aim is to recognize the gradients of high magnitude and scale it at various stage in such a way that large gradients have to be suppressed by high magnitude whereas low gradients by low magnitude.

$$l(x,y) = \nabla m(x,y)n(x,y), \tag{18}$$

where $H(x,y) = log(I(x,y))$ and $n(x,y)$ is the attenuation function which is discussed later. In our method, we use a direct method for finding the potential function which is minimized by the function $P(x,y)$. In other words, $P(x,y)$ should minimize the following integral

$$\int\int h\left(\nabla P, l\right) dxdy, \tag{19}$$

where $h\left(\nabla P, l\right) = \|\nabla P - l\|^2 + f(\nabla P(x,y))$. Using Euler-Lagrange equation, we can find out the $P(x,y)$ which minimizes the Eq. 19. The second term in right hand of Eq. 19 is called as regularizer term. For the better selection of regularizer function as discussed above, we have taken two choices

$$f_1(t) = \sqrt{1+t^2}. \tag{20}$$

$$f_2(t) = \frac{t^2}{1+t^2}. \tag{21}$$

This satisfies all the conditions which it requires, that have been discussed in the previous section. We have used only f_2 regularizer for which the solution can be given in Eq. 22.

$$h\left(\nabla P, l\right) = \|\nabla P - l\|^2 + \lambda\frac{(\nabla P(x,y))^2}{1+(\nabla P(x,y))^2} \tag{22}$$

$$\frac{\partial h}{\partial P} - \frac{d}{dx}\frac{\partial h}{\partial P_x} - \frac{d}{dy}\frac{\partial h}{\partial P_y}. = 0 \tag{23}$$

Putting the value of h in the Eq. 23 and solving it we get

$$\nabla^2 P - div(l) + \lambda\frac{\nabla^2 P}{(1+(\frac{\partial p}{\partial x})^2 + (\frac{\partial P}{\partial x})^2)^3} = 0, \tag{24}$$

where $\nabla^2 P = \frac{\partial^2 P}{\partial x^2} + \frac{\partial^2 P}{\partial y^2}$ and $divl = \frac{\partial l_x}{\partial x} + \frac{\partial l_y}{\partial y}$. Here, we have taken the results on the various value of λ and showed how it achieves convexity.

4.1 Implementation

In order to get the solution for P, we have used difference method. So, we can write

$$\nabla^2 P \approx P(x+1,y)+P(x-1,y)+P(x,y+1)+P(x,y-1)-P(x,y),$$

$$divl = \left(l_x(x,y) - l_x(x-1,y), l_y(x,y) - l_y(x,y-1)\right),$$

$$\nabla P = \left[P(x+1,y) - P(x,y), P(x,y+1) - P(x,y)\right].$$

Using finite difference method, we are representing the distinct terms discussed above. This finite difference method (FDE) generates a very large system of linear equations. There will be one equation for every pixel of the image but in the corresponding matrix there are only five non-zero elements in every row, rest are zeros because each pixel is coupled with its only four neighbours. Full Multigrid Algorithm has been used with Gauss-Seidal iterations. This method operates on the luminance value of the image. After an operation on luminance, the luminance has to be replaced by the new luminance value P, in our case. More clearly, we can say the colour channel can be replaced by the following equation

$$[R,G,B]out = \left(\frac{[R,G,B]_{in}}{L_{in}}\right)^s L_{out}, \tag{25}$$

where the value of s is varied from 0.4 and 0.6.

4.2 Quality Parameters

The presence of overexposed and underexposed regions make quite difficult to quantify the quality of the image by any particular quantitative measure. However, in the image processing algorithm, we always try to enhance the local contrast. So, contrast enhancement factor [25] becomes very much important quantitative parameter as far as visuality is concerned.

Contrast Enhancement Factor (CEF): It is defined as the ratio of variance and mean of the image.

$$CEF = \frac{\sigma^2}{\mu} \tag{26}$$

The high local variance value represents the high contrast image.

5. RESULTS & DISCUSSION

We have experimented our proposed technique on various high dynamic range images of real scenes. We have taken the

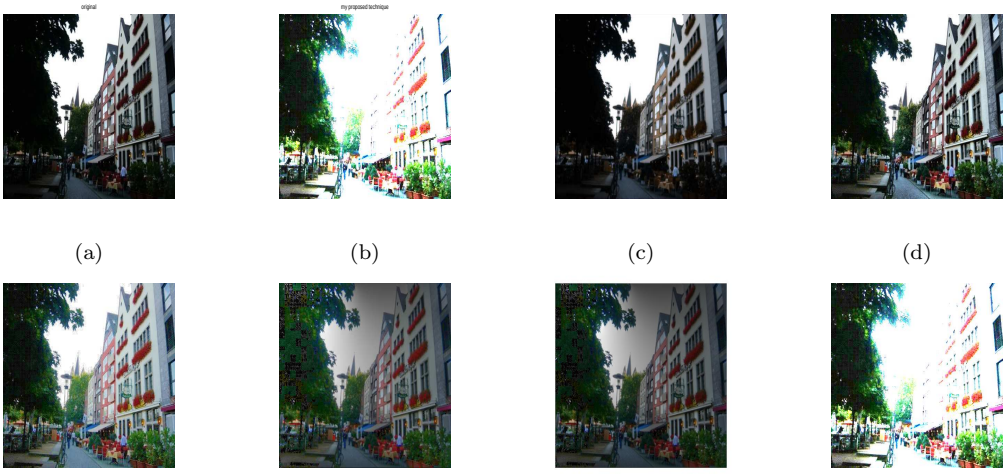

(a) (b) (c) (d)

(e) (f) (g) (h)

Figure 3: (a) Input Image 1 (b) Proposed Method (c) Anisotropic Diffusion (d) CLAHE Output (e) HE (f) Regularizer (g) [10] Output (h) DSR + DWT

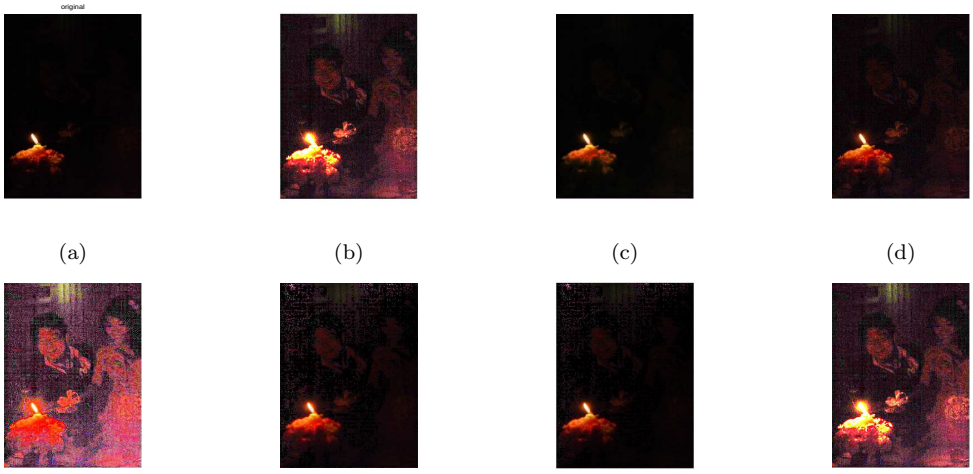

(a) (b) (c) (d)

(e) (f) (g) (h)

Figure 4: (a) Input Image 2 (b) Proposed Method (c) Anisotropic Diffusion (d) CLAHE Output (e) HE (f) Regularizer (g) [10] Output (h) DSR + DWT

(a) 13a (b) (c) (d)

(e) (f) (g) (h)

Figure 5: (a) Input Image 3 (b) Proposed Method (c) Anisotropic Diffusion (d) CLAHE Output (e) HE (f) Regularizer (g) [10] Output (h) DSR + DWT

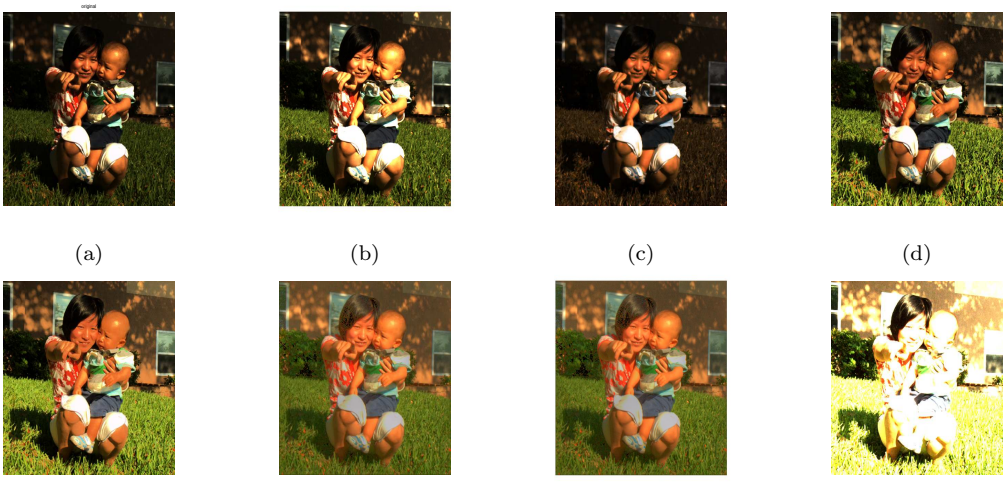

(a) (b) (c) (d)

(e) (f) (g) (h)

Figure 6: (a) Input Image 4 (b) Proposed Method (c) Anisotropic Diffusion (d) CLAHE Output (e) HE (f) Regularizer (g) [10] Output (h) DSR + DWT

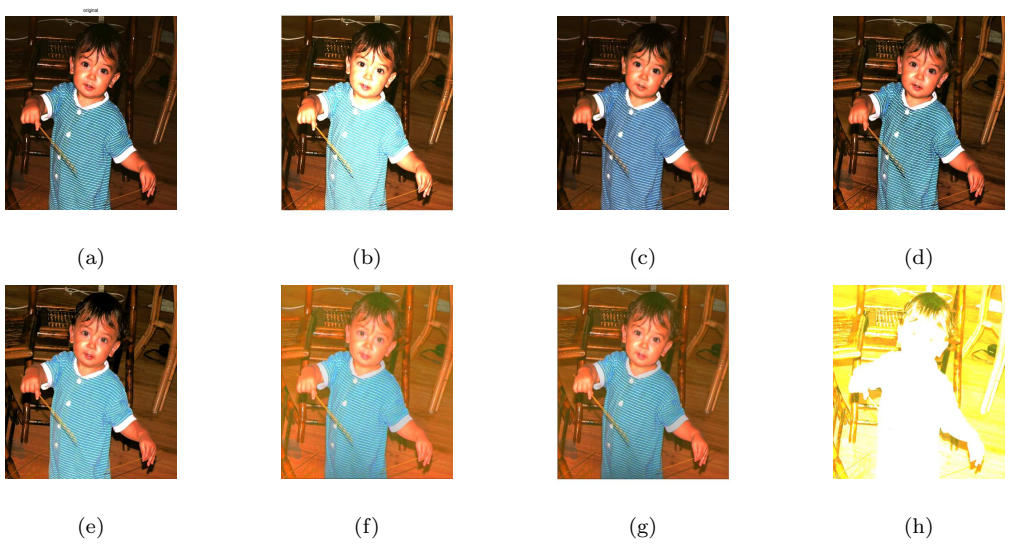

(a) (b) (c) (d)

(e) (f) (g) (h)

Figure 7: (a) Input Image 5 (b) Proposed Method (c) Anisotropic Diffusion (d) CLAHE Output (e) HE (f) Regularizer (g) [10] Output (h) DSR + DWT

Contrast Enhancement Factor								
Input Images	No Filter	HE	CLAHE	AD	DSR + DWT	Regularizer	[10] method	Proposed method
Input Image 1	14.1923	36.8897	24.9312	13.7761	53.2421	31.1472	22.6889	50.2749
Input Image 2	25.9608	84.0375	35.3544	25.1274	61.9123	39.1057	30.3328	55.9945
Input Image 3	39.3199	93.8785	64.3705	38.8927	87.9972	70.2443	46.6344	95.4648
Input Image 4	53.0426	82.7405	70.0349	51.4951	84.6170	74.5434	74.5434	65.6728
Input Image 5	68.7929	88.3480	78.0000	67.2930	112.1171	122.0620	99.7288	80.5883

Table 1: Comparative study of different existing filter, where HE, CLAHE and AD stands for Histogram Equalization, Contrast Limiting Adaptive Histogram Equalization and Anisotropic Diffusion respectively

images from [26, 27]. In almost all cases, our proposed technique gives satisfactory outcomes without much parameter alteration. Here, five different test images, which have different radiance map have been taken and corresponding output with respect to f_2 as regularizer has been shown. Regularizer has been applied to gradient compression method for overexposed region whereas DSR has been applied on the LL band of the underexposed region. In Fig. 3, results have been compared to some known filters. Fig. 3b is comparable to all other techniques visually. It can also be seen verified by the Table 1, where CEF (50.2749) of our technique is greater than all except ($CEF = 53.2421$) of $DSR{+}DWT$. In Fig. 4, input image contain fully dark background with some pixels of light. In this technique our result 4b ($CEF = 55.9945$) is better or comparable to others except 4e ($CEF = 84.0375$). The Fig. 5 shows a lady in the kitchen with high underexposed regions. Fig. 5b ($CEF = 95.4648$) is better than all the techniques. In the Fig. 6 the visuality of our proposed technique 6b ($CEF = 65.6728$) is better compared to AD 6c ($CEF = 51.4951$) only. In the last input image which is shown in Fig. 7, our method, Fig. 7b ($CEF = 80.5883$) gives better than AD ($CEF = 67.2930$) $ CLAHE ($CEF = 78.0000$).

6. CONCLUSION AND FUTURE WORK

In this paper, we present a new regularizer based approach for correcting the pixels which are affected by the under and overexposure in the input photograph. Our numerical approach method is appropriate for improvement of overexposed and underexposed regions than some other existing technique. We have made a comparative analysis between the result of [10] and our proposed technique. The performance of the result for better convergence depends upon λ. There are few issues which can be discussed very clear that unfaithful color can be produced near the boundary of overexposed regions. Small halo-like artifacts can not be dealt using this approach because of the incapability for this mechanism. Future work will be more focused on recovery of an image using modified gradient fields.

7. REFERENCES

[1] J. W. Harris, and H. Stocker. Handbook of Mathematics and Computational Science. *Springer-Verlag*, 1998

[2] D. J. Jobson, Z. Rahman, and G. A. Woodell. A multi-scale Retinex for bridging the gap between color images and the human observation of scenes. *IEEE Trans. on Image Processing* 6, July, 1997.

[3] E. H. Land , and J. J. Mccann. Lightness and Retinex theory. *Journal of the Optical Society of America* 61, Jan, 1971.

[4] R. K. Jha, R. Chouhan, K. Aizawa, and P. K. Biswas. Dark and low-contrast image enhancement using

dynamic stochastic resonance in discrete cosine transform domain. APSIPA Trans. on Signal and Information Processing, vol. 2, 2013.

[5] R. Chouhan, R. K. Jha, and P. K. Biswas. Enhancement of dark and low-contrast images using dynamic stochastic resonance. *IET Image Processing*, vol. 7, 2013.

[6] X. Zhang and D. H. Brainard. Estimation of saturated pixel values in digital color imaging. *Journal of the Optical Society of America* 21(12):2301-2310, 2004.

[7] S. Z. Masood, J. Zhu, and M. F. Tappen. Automatic correction of saturated regions in photographs using crosschannel correlation. *In Proc. Pacific Conference on Computer Graphics and Applications*, 2009.

[8] L. Wang, L.Y.Wei, K. Zhou, B. Guo, and H. Y. Shum. High dynamic range image hallucination. *In Proc. EGSR*, 2007.

[9] H.T. Chen, T.L. Liu, and T.L. Chang. Tone reproduction: A perspective from luminance-driven perceptual grouping. *In Proc. CVPR*, 2005.

[10] R. Fattal, D. Lischinski, and M. Werman. Gradient domain high dynamic range compression. *ACM Trans. Graphics*, 21(3):249-256, 2002.

[11] E. Reinhard, M. Stark, P. Shirley, and J. Ferwerda. Photographic tone reproduction for digital images. *ACM Trans. Graphics*, 21(3):267-276, 2002.

[12] P. Getreuer. Automatic Colour Enhancement (ACE) and Its Fast Implementation. *Image Processing On Line (IPOL)*, 2012.

[13] J. L. Lisani, A. B. Petro, and C. Sbert. Colour and Contrast Enhancement by Controlled Piecewise Affine Histogram Equalization. *Image Processing On Line (IPOL)*, 2012.

[14] P. Perez, M. Gangnet, and A. Black. Poisson image editing. *ACM Trans. Graphics*, vol 22, pp. 342- 348, 2003.

[15] T. F. Chan and J. Shen. Mathematical models for local nontexture inpaintings. *SIAM J. Appl. Math*, 62, pp. 1019-1043, 2002.

[16] T. F. Chan, J. Shen, and H. M. Zhou. Total variation wavelet inpainting. *J. Math. Imaging Vision*, 25, pp. 107-125, 2006.

[17] A. Criminisi, P. Patrick, and T. Kentaro. Region filling and object removal by exemplar-based image inpainting. *IEEE Trans. Image Process.*, 13, pp. 1200-1212, 2004.

[18] M. Aggarwal and N. Ahuja. High dynamic range panoramic imaging. *In Proc. IEEE ICCV*, vol. I, 2-9, 2001.

[19] S. Geman and D. Geman. Stochastic relaxation, Gibbs distribution and the bayesian restoration of images. *IEEE Trans. Pattern Anal. Machine Intell.*, vol. 6, pp. 721-741, 1984.

[20] A. N. Tikhonov and V. Y. Arsenin. Solutions of Ill-Posed Problems. Wiley, New York, 1977.

[21] G. Aubert, and L. Vesea. Variational Method In Image Recovery. *Society for Industrial and Applied Mathematics*, vol. 34, 1997.

[22] P. Charbonnier, L. Blanc-Feraud, G. Aubert, and M. Barlaud. Deterministic edgepreserving regularization in computed imaging. *IEEE Trans. Image Processing,* pp. 298-311, 1997.

[23] R. Benzi, A. Sutera and A. Vulpiani. The mechanism of stochastic Resonance. *J. Phys. A: Math. Gen*, vol. 14, pp. L453-L457, 1981.

[24] http://www.wavelet.org/tutorial/wbasic.htm.

[25] J. Mukherjee, and S. K. Mitra. Enhancement of Color Images by Scaling the DCT Coefficients. *IEEE Trans. Image Processing,* vol. 17, No. 10, 2008.

[26] http://robotics.pme.duth.gr/phos2.html.

[27] http://www.cs.ucf.edu/ smasood/research.html.